Cell Tissue Res (2011) 345:137–148
DOI 10.1007/s00441-011-1182-x

REGULAR ARTICLE

Dynamics of expression of ARID1A and ARID1B subunits in mouse embryos and in cells during the cell cycle

Angel Flores-Alcantar · Adriana Gonzalez-Sandoval · Diana Escalante-Alcalde · Hilda Lomelí

Received: 26 November 2010 / Accepted: 19 April 2011 / Published online: 7 June 2011

Abstract The mammalian SWI/SNF chromatin remodeling complexes play essential roles in cell cycle control through the transcriptional regulation of cell-cycle-specific genes. These complexes depend on the energy of ATP hydrolysis provided by the BRG1 or BRM catalytic subunit. They contain seven or more noncatalytic subunits, some being constitutive components, with others having paralogs that assemble in a combinatory manner producing different SWI/SNF-related complexes with specific functions. ARID1A and ARID1B are mutually exclusive subunits of the BAF complex. The specific presence of these subunits in the complex has been demonstrated to determine whether SWI/SNF functions as a corepressor (ARID1A) or as a coactivator (ARID1B) of the cell cycle genes. Our aim has been to analyze the relevance of the ARID1 subunits in development. We have compared the patterns of expression of these two genes through various mouse embryonic stages. *Arid1a* is expressed widely and intensively, whereas *Arid1b* is poorly transcribed and expressed in selected regions. Moreover, ARID1A and ARID1B present different kinetics of expression in the cell cycle. ARID1A accumulates in G0 and is downregulated throughout the cell cycle phases but is completely eliminated during mitosis, whereas ARID1B is expressed at comparable levels at all phases, even during mitosis. These kinetics probably affect the incorporation patterns of the ARID1 proteins to the complex and hence modulate SWI/SNF activity during proliferation and arrest.

Keywords ARID · Chromatin remodeling · Cell cycle · Developmental expression · BAF complex · Mouse (CD1)

Introduction

Chromatin remodeling complexes are epigenetic modifiers that alter the structure of chromatin and change its accessibility to transcriptional regulators. Switch/sucrose nonfermentable (SWI/SNF) is a class of chromatin-remodeling complex that utilizes the energy of ATP hydrolysis and is composed of several subunits that are combined differently to produce distinct SWI/SNF-like complexes. The central component of such complexes is a subunit that posses ATPase activity. In vertebrates, two alternative ATPases associate to SWI/SNF, viz., brahma-related gene 1 (BRG1) and Brahma protein (BRM). In addition to this catalytic subunit, the SWI/SNF family shares at least seven other common proteins and can be distinguished by the presence of additional unique subunits (Martens and Winston 2003; Mohrmann and Verrijzer 2005). Differences in subunit composition produce functional diversity and allow biological specificity (Ryme et al. 2009).

According to their composition, two main SWI-SNF-like complexes have been identified in mammalian cells: BAF and PBAF, which differ in their largest subunit. The signature subunit for BAF is ARID1, while those for PBAF are BAF180 plus BAF200/ARID2 (Wang 2003; Mohrmann

This work was supported by DGAPA-UNAM grant IN220009-3 and CONACyT 49114.

A. Flores-Alcantar · A. Gonzalez-Sandoval · H. Lomelí (✉)
Departamento de Genética del Desarrollo y Fisiología Molecular,
Instituto de Biotecnología,
Universidad Nacional Autónoma de México,
Mexico City, Mexico
e-mail: hilda@ibt.unam.mx

D. Escalante-Alcalde
División de Neurociencias, Instituto de Fisiología Celular,
Universidad Nacional Autónoma de México,
Ciudad Universitaria,
Mexico City, Mexico

and Verrijzer 2005). ARID1A and ARID1B are two subunits that exist as a mutually exclusive pair and define two functional variants of the BAF complex (Wang et al. 2004b). The ARID1 proteins share more than 60% identity across their entire lengths. Their most prominent feature is the presence of an ARID DNA-binding domain, which shows no preference for any DNA sequence (Dallas et al. 2000; Hurlstone et al. 2002; Kozmik et al. 2001; Nie et al. 2003).

ATP-dependent remodeling is known to play an important role in regulating the balance between proliferation and differentiation. Previous evidence has specifically implicated the BAF complex in cell cycle regulation (Nagl et al. 2005, 2006). In vitro studies of the MC3T3-E1 preosteoblasts line have demonstrated that the choice between ARID1A and ARID1B produces assemblies with opposite effects on the cell cycle: during reversible cell cycle arrest induced by deprivation of serum, ARID1A-based complexes are required for arrest, whereas once serum is restored, the participation of ARID1B-based complexes is essential for resuming cell cycle activity. These activities are correlated with the formation of anti-proliferative- or pro-proliferative-specific complexes that associate to promoters of specific cell cycle genes (Nagl et al. 2007). The mechanisms that operate to regulate the dynamics of the assembly of the alternative ARID1 subunits into the SWI/SNF complex in order to regulate its function remain undefined.

The relevance of the ARID1 proteins in vivo has been analyzed during pre-implantation and early development. Loss of ARID1A function leads to developmental arrest around 6.5 days post coitum (dpc) and compromises pluripotency and self-renewal of embryonic stem (ES) cells (Gao et al. 2008). On the other hand, the inactivation of ARID1B in ES cells causes a reduced proliferation rate and an abnormal cell cycle, suggesting that ARID1B is also involved in cell cycle regulation in vivo (Yan et al. 2008).

According to one report, ARID1A is present at higher levels compared with ARID1B in a variety of tumor cell lines (Wang et al. 2004a). In contrast, a more recent study suggests that, upon differentiation of ES cells, RNA levels of ARID1A decrease, whereas those of ARID1B increase, thereby identifying the former as the predominant subunit in pluripotent cells and the latter as a differentiated cell-type subunit (Kaeser et al. 2008; Yan et al. 2008). In vivo, the expression patterns of ARID1A and ARID1B in mouse embryos have not been compared directly.

In this work, we have investigated the detailed gene expression pattern of the *Arid1* genes in developing embryos from pre-implantation to mid-stages. We have found that, both at the transcript and protein levels, ARID1A is abundantly expressed and broadly distributed in the embryo at all stages analyzed, showing that this subunit is not specific for pluripotential cells and suggesting that it plays a more ubiquitous role than ARID1B in SWI/SNF activity during development. We have also followed the dynamics of the expression of the ARID1 proteins at various phases of the cell cycle in the MC3T3-E1 preosteoblast cell line, embryonic stem cells, and preimplantation embryos. We show that ARID1A presents a similar kinetics to that previously reported for BRM, being degraded at mitosis (Muchardt et al. 1996), whereas ARID1B maintains a constant protein level during mitosis, as previously shown for BRG1 (Muchardt et al. 1996). Our analysis also indicate that, in embryos, higher molecular weight isoforms are produced for both ARID1 proteins, and that their presence is variable throughout development. For ARID1A, we have detected that this larger species is ubiquitinated ARID1A suggesting that this covalent modification is relevant for ARID1 function in vivo.

Materials and methods

Embryo collection

Mouse embryos were collected from time-mated females of the CD1 out-bred strain, with noon of the day in which the mating plug was observed being designated 0.5 dpc. Pregnant females were sacrificed by cervical dislocation. For pre-implantation stages, embryos were recovered from the oviduct (morulas) or uterus (blastocyst) by extremely gentle flushing with M2 medium (Specialty Media, Phillipsburg, N.J., USA), under a dissection microscope.

Probe preparation

Arid1a and *Arid1b* riboprobes were transcribed in vitro from pCRII-TOPO constructs. The *Arid1a* insert included 861 nucleotides (positions 1196–2056 of the coding sequence), whereas the *Arid1b* insert contained 701 nucleotides (positions 4201–4892 of the coding sequence). The plasmid-constructs were linearized with *Bam*HI for antisense probes and transcribed with digoxigenin RNA labeled mix and T7 RNA polymerase (Roche). For the sense probes, the constructs were linearized with *Hin*dIII and transcribed with Sp6 RNA polymerase (Roche).

Whole-mount RNA in situ hybridization

Whole embryos were fixed overnight in 4% paraformaldehyde (PFA) at 4°C and dehydrated in a graded methanol series prior to storage at –20°C. Whole-mount in situ hybridization (ISH) was performed as described previously (Hogan et al. 1994). Briefly, embryos were rehydrated in a graded methanol series and treated with proteinase K (10 μg/ml; Invitrogen). Embryos were post-fixed with

0.2% glutaraldehyde/4% PFA and washed in PBT (0.1% Tween-20/phosphate-buffered saline [PBS]) prior to hybridization overnight at 68°C. Embryos were washed twice in 2× standard sodium citrate (SSC)/0.2% SDS at 70°C, followed by two identical washes in 0.2× SSC/0.2% SDS. Embryos were incubated overnight with anti-digoxigenin antibody (Roche) at 4°C, and after several washes with TBS-T (50 mM TRIS-buffered saline pH 7.5, 0.05% Tween-20), color was developed by using nitroblue tetrazolium/5-bromo-4-chloro-2-indolyl-phosphate (Roche).

Cell culture and synchronization

Low-passage MC3T3-E1 cells (MC3T3 E1; cat. CRL-2593, ATCC, USA) were grown in α-MEM plus 10% fetal bovine serum (FBS) supplemented with 100 mM β-mercaptoethanol, 50 units/ml penicillin, and 50 μg/ml streptomycin (Gibco; Sigma). For serum depletion, monolayers at 70% confluency were washed in PBS, incubated 72 h in α-MEM, 0.1% FBS (Nagl et al. 2007). For S-phase block, serum-depleted cells were stimulated for 5 h in fresh medium (α-MEM, 10% FBS), hydroxyurea (Sigma) was added at a concentration of 1 mM for 18 h, and the cells were released in fresh medium for 3 h. For G2/M synchronization, hydroxyurea-blocked cells were washed three times with PBS and released into fresh medium for 5 h. Then, 60 μg/ml colchicine (Sigma) was added, and the cells were incubated for 24 h. Mitotic cells were subsequently harvested by gentle pipetting (shake off).

For ES cell culture, W9.5 cells were grown on a feeder layer with DMEM (GIBCO) plus 15% FBS for 48 h. Semi-confluent 10-cm dishes were lysed for protein experiments and for immunofluorescence (IF).

Flow cytometry

Cells were treated for 2 min with 0.25% trypsin, washed twice in PBS, and fixed for 30 min in 70% ethanol. Cells were then re-hydrated with PBS, treated for 1 h with RNAse (50 U, Roche) in staining buffer (100 mM TRIS-HCl pH 7.4, 150 mM NaCl, 1 mM $CaCl_2$, 0.5 $mMgCl_2$, 0.1% NP-40). Sytox-green staining (0.5 μM; Invitrogen) was performed at 37°C for 30 min. Cells were analyzed with a FACSort with CellQuest (BD Biosciences) and FlowJo software.

Western immunoblotting

Protein extracts were obtained from cells and embryos (8.5–10.5 dpc). The samples were homogenized in Triton lysis buffer (TLB: 20 mM TRIS pH 7.4, 137 mM NaCl, 25 mM β-glycerolphosphate pH 7.4, 2 mM sodium pyrophosphate, EDTA pH 7.4, 1% Triton X-100, 10% glycerol, and the following protease inhibitors: 1 mM phenylmethane sulfonyl-fluoride, 5 ug/ml Leupeptin, 5 ug/ml Antipain, 5 ug/ml Aprotinina, 5 ug/ml Pestatin A, 0.5 mM dithiothreitole, 200 mM $NaVO_4$) at 4°C for 2 h, centrifugated at 14,000 rpm for 10 min, and stored at −20°C. Proteins were quantified with the Bradford assay method (BioRad, Richmond, Calif., USA). Each protein sample (100 μg) was resolved by SDS–polyacrylamide gel electrophoresis (SDS-PAGE; 7%) and transferred to 0.45-μm nitrocellulose membranes (Bio-Rad), which were blocked with 5% non-fat milk in TBS-T and incubated with the indicated antibody diluted in TBS-T with 5% non-fat milk. After three washes with TBS-T, membranes were incubated with the second antibody (anti-rabbit for anti-β tubulin or anti-mouse for the ARID1 antibodies) coupled to horseradish peroxidase (HRP), and proteins were visualized with LumiGLO reagent (Cell Signaling Technology), following the manufacturer's instructions. Anti-ARID1A (sc-32761), anti-ARID1B (sc-32752), anti-β-tubulin (sc-9104), anti-mouse IgG-HRP (sc-2055), and goat anti-rabbit IgG-HRP (sc-2004) were purchased from Santa Cruz Biotechnology. As a molecular weight marker the Page Ruler Plus Pre-stained Protein Ladder (Fermentas) was used.

Endogenous immunoprecipitation

ES cells were harvested and collected by centrifugation at 1000 rpm for 5 min. The cells were lysed in five pellet volumes of TLB or TLB plus 10 mM N-ethylmaleimide (NEM) at 4°C for 2 h. The extract was centrifuged for 10 min at 14,000 rpm in a microfuge. Total protein extract (1 mg) was incubated with 1 μg of the indicated antibodies (ARID1A or Ubiquitin; SIGMA U5379) at 4°C for 1.5 h, after which 100 μl of a 50% Protein A/G Sepharose slurry was added, and the samples were incubated for an additional hour at 4°C. The beads were washed twice with 200 μl wash buffer (25 mM HEPES pH 7.6, 0.1 M KCl, 12.5 mM $MgCl_2$, 0.1 mM EDTA, 20% v/v glycerol, and complete mix proteinase inhibitors from ROCHE), resuspended in 100 μl sample buffer, and separated on a 7% SDS–polyacrylamide gel by SDS-PAGE. The negative control included the reaction carried out without the antibody.

Immunofluorescence

Pre-implantation embryos were treated with acid Tyrode solution in order to remove the zona pellucida. Embryos and cells were fixed for 30 min at room temperature in methanol:dimethylsulfoxide (4:1), washed three times in PBS, and blocked for 1 h at room temperature with 2% non-fat milk plus 0.05% Tween-20 in PBS. Samples were incubated overnight at 4°C with primary antibodies diluted in blocking solution: anti-ARID1A (sc-32761 Santa Cruz Biotech; 1:100) and anti-Ser10 phosphorylated histone 3

(H3S10P; Santa Cruz Biotech; 1:1000) or anti-proliferating cell nuclear antigen (PCNA; sc-7907 Santa Cruz Biotech; 1:1000), or anti-ARID1B (H00057492-M02 Abnova; 1:100) and anti-H3S10P or anti-PCNA. Next morning, the embryos were washed three times in PBS and incubated 1 h at room temperature in secondary antibodies: Alexa fluor 488 conjugated to anti-rabbit IgG and Alexa fluor 647 conjugated to anti-mouse IgG (Invitrogen). Embryos were washed and mounted with PBS on slides. The cells were washed and mounted in 90% glycerol.

Confocal laser scanning microscopy

Images were obtained by a LSM 510 meta confocal microscopy with a 63× W N.A. 1.2 objective (Zeiss, Germany). A BP 500–530 IR filter and a laser Ar 488-nm excitation wavelength were used for the detection of Alexa fluor 488 anti-rabbit IgG and BP 650–710 IR and laser HeNe 633-nm excitation wavelength were used for the detection of Alexa fluor 647 anti-mouse IgG. Serial optical sections were produced at 2 μm as the Z-step.

Fluorescence data analysis

Each quantification involved three independent experiments, and at least 40 nuclei were analyzed per experiment. Image acquisition was performed by maintaining the settings during the complete session for comparison purposes. Complete embryos were visualized by using optic slides in the Z-axis, whereas cells were captured in one shot. Measurements were carried out by using the public domain NIH ImageJ 1.41o program. Fluorescence quantification for embryos was undertaken by including half of the total area (from center to top). The average of pixels in three optic slides was obtained for individual nuclei. The mean of pixels (gray level threshold, 256 colors) of all nuclei in the sample was considered as the relative level of expression. The level of expression of H3S10P grouped three populations: interphasic (0–5 pixels [px]), prophasic (6–30 px), and advanced mitotic (above 30 px), which were confirmed by morphological criteria. The quantification of PCNA generated two groups (0–20 px and above 20 px). The ARID1A or ARID1B signal was compared among these groups. Statistical analysis (Student *t*-tests) was carried out with Excel and Prism software.

Results

Comparative expression of ARID1 genes in the embryo

Whole-mount ISH analyses of 7.5-dpc to 10.5-dpc embryos was performed with a probe used for the detection of *Arid1a*; the probe hybridizes with the two reported splicing forms of this gene (Kozmik et al. 2001). All the ISH assays carried out with the *Arid1a* probe were developed for 6 h. With this probe, a strong signal was detected at 7.5 dpc. The expression was ubiquitous including extra-embryonic regions (Fig. 1a). Sections of an *Arid1a*-probed embryo showed intensive expression in all germ layers, although the maximal intensity was detected along the primitive streak (Fig. 1b). At 8.5 dpc, we still found strong and nearly ubiquitous expression of *Arid1a*. The most conspicuous sites of expression were the posterior neural plate, brain, and the somites (Fig. 1c, d). Some regions in the embryo did not show expression of this gene, for example, around the midline in the brain region, in the atrial chamber of the heart, and in intersomitic tissue (Fig 1c, d). At 9.5 dpc, the *Arid1a* probe detected a strong signal in the ectoderm-derived tissues and mesenchyme. Interestingly, in whole embryos, no signal was detectable in endoderm-derived organs and the heart (Fig. 1e). Parasagittal sections revealed expression in the head mesenchyme, neural tissues, and somites (Fig. 1f). The expression of *Arid1a* seems to decline at 10.5 dpc but remaining in the forebrain and hindbrain, somites, limbs, branchial arches, and tailbud (Fig. 1g). Significantly, the midbrain did not exhibit *Arid1a* transcripts at this stage.

In contrast to the strong signal observed with the *Arid1a* probe, *Arid1b* transcripts were detected in whole-mount 7.5-dpc embryos only after development of the color for 40 h and were visible in the neuroectoderm, mesoderm, and chorion (Fig. 2a, b). Sections of these embryos revealed that the maximal intensity of signal was present in the mesoderm, but that signal also occurred in the distal epiblast and the visceral endoderm (Fig. 2b). At 8.5 dpc, embryos probed with *Arid1b* required, once again, an extremely long exposure to substrate in order to display a poor signal. Moreover, differently from observations for *Arid1a*, the pattern of expression of *Arid1b* was restricted to neural tissue, including the neural crest, forebrain, and posterior neural plate (Fig. 2c, d). At 9.5 dpc, *Arid1b* transcripts were clearly detected in the ventral regions of the embryo and absent in the dorsal part and in the brain (Fig. 2e). A parasagittal section of this embryo demonstrated that the highest levels of expression were found in the branchial arches, optic vesicle, head and trunk ventral mesenchyme, and intestine (Fig. 2f). *Arid1b* also appeared to be downregulated at 10.5 dpc with transcripts remaining mainly in the optic and otic vesicles (Fig. 2g).

The more obvious detection of *Arid1a* in embryos suggests that it is more abundantly expressed compared with *Arid1b*. To analyze this possibility further, we performed Western blots to detect both ARID1 proteins in extracts of 8.5-, 9.5-, and 10.5-dpc embryos and in ES cells included as a reference of early development. For these

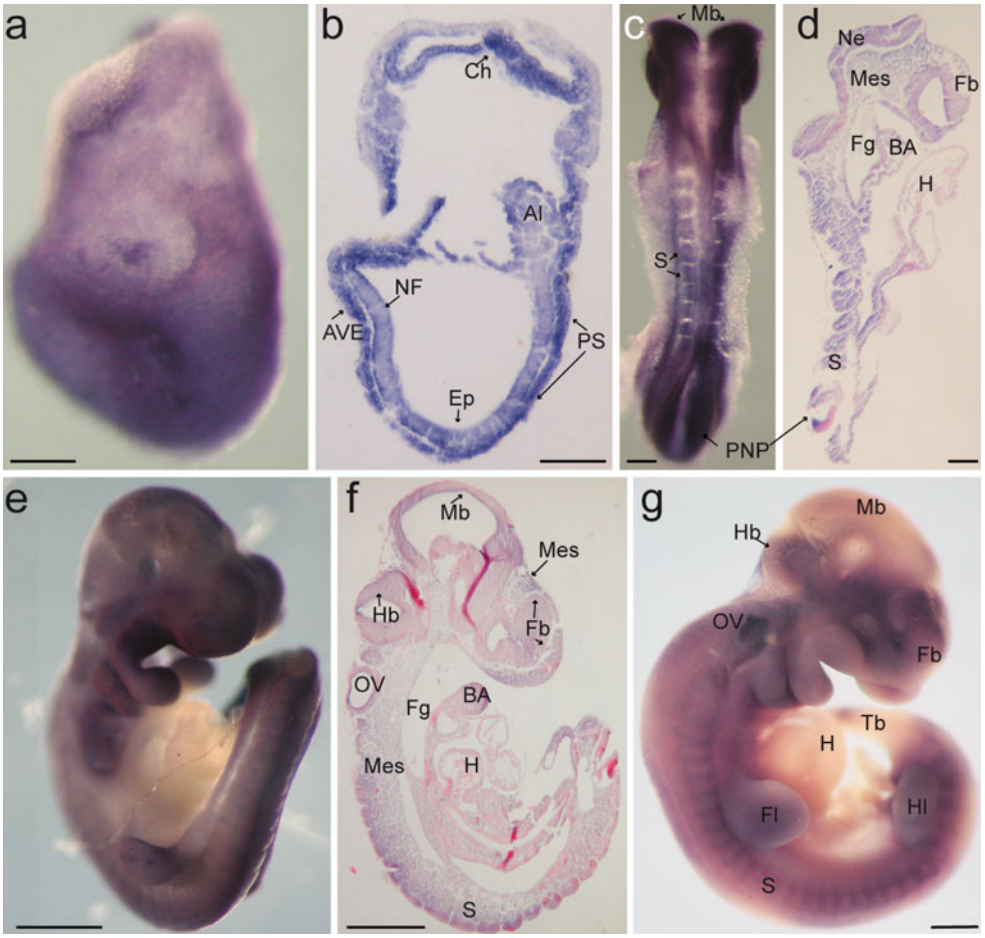

Fig. 1 Expression of *Arid1a* at embryonic stages 7.5 dpc to 10.5 dpc. **a**, **c**, **e**, **g** Whole-mount in situ hybridization (ISH) of 7.5 dpc (**a**), 8.5 dpc (**c**), 9.5 dpc (**e**), and 10.5 dpc (**g**) embryos probed for *Arid1a*. Sagittal histological sections at a midline level of embryos in **a**, **c**, **e** are shown in **b**, **d**, **f**, respectively (*Al* alantois, *AVE* anterior visceral endoderm, *BA* branchial arches, *Ch* chorion, *Ep* epiblast, *Fb* prospective forebrain, *Fg* foregut, *Fl* forelimb, *H* heart, *Hb* hindbrain, *Hl* hindlimb, *Mb* midbrain, *Mes* mesenchyme, *NF* neural fold, *PNP* posterior neural plate, *OV* otic vesicle, *PS* primitive streak, *S* somites, *Tb* tailbud). In **a**, **b**, anterior is *left*. **c** Dorsal view. **f** Section counterstained with eosin. *Bars* 100 μm (**a-d**) 500 μm (**e-g**).

experiments, we used commercial monoclonal antibodies whose signals were previously shown to be proportional to the respective amounts of ARID1A and ARID1B purified glutathione-S-transferase-fusion proteins (Wang et al. 2004b), and quantification involved normalization to β-tubulin levels. Western blots comparing the protein levels of these subunits confirmed that, in general, ARID1A was more abundant compared with ARID1B, both in the embryonic extracts and in the ES cells (Fig. 3a, b). However, ARID1A exhibited increased expression in ES cells (Fig. 3a, c), in agreement with previous results indicating that, upon the differentiation of these cells, the *Arid1a* gene is downregulated (Kaeser et al. 2008; Yan et al. 2008). In contrast, the protein level of ARID1B was not increased during developmental differentiation, as was suggested by Kaeser et al. (2008), and is indeed barely detected in embryos (Fig. 3a, b). Another important observation revealed by the quantification was that, at 10.5 dpc, ARID1A was as abundant as in previous stages, indicating that the perception of transcriptional down-regulation that emerged from the ISH was not reflected at the protein level. Both antibodies detected at least two bands: one that probably represented the full-length protein (239–242 kDa) and one that migrated slower and was suggestive of covalent modifications (>270 kDa). Interestingly, the 270-kDa species was more abundant for both proteins in embryonic extracts. Moreover, for ARID1A, we found that the relative amounts of these two species could be reproducibly associated to the developmental stages (Fig. 3a, c): in ES cells, the relative amounts of the unmodified protein versus the putative modified protein was similar, whereas in the embryos at midgestation, the unmodified protein was present at an extremely low concentration compared with the putative modified species, which was largely predominant.

Altogether the results obtained from the ISH and immunoblot assays indicate that although ARID1A is downregulated in embryos, it is still very strongly expressed in differentiated cells, both at the transcript level and at the protein level; on the other hand, ARID1B is constantly expressed at similar low levels in all developmental stages analyzed.

ARID1A is post-translationally modified by ubiquitin in vivo

To investigate further the nature of the shift band of ARID1A detected through immunoblotting, we next

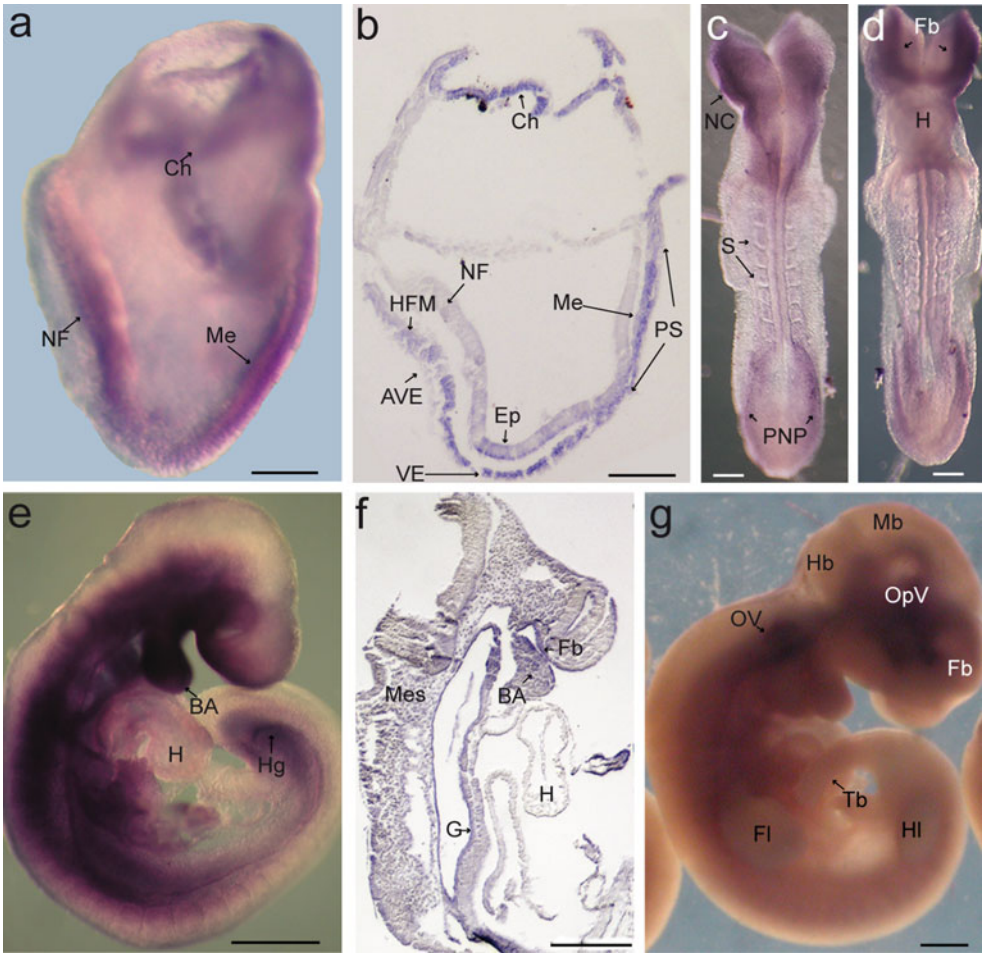

Fig. 2 Expression of *Arid1b* at embryonic stages 7.5 dpc to 10.5 dpc. **a**, **c–e**, **g** Whole-mount ISH of 7.5 dpc (**a**), 8.5 dpc dorsal (**c**), and ventral (**d**) views, 9.5 dpc (**e**) and 10.5 dpc (**g**) embryos probed for *Arid1b* (*AVE* anterior visceral endoderm, *BA* branchial arches, *Ch* chorion, *Ep* epiblast, *Fb* forebrain, *Fl* forelimb, *G* gut, *H* heart, *Hb* hindbrain, *HFM* headfold mesenchyme, *Hg* hindgut, *Hl* hindlimb, *Mb* midbrain, *Me* mesoderm, *Mes* mesenchyme, *NC* neural crest, *NF* neural fold, *OV* otic vesicle, *OpV* optic vesicle, *PNP* posterior neural plate, *PS* primitive streak, *S* somites, *Tb* tailbud, *VE* visceral endoderm). Sagittal histological sections at a midline level of embryos in **a**, **e** are shown in **b**, **f**, respectively. In **a**, **b**, anterior is *left*. *Bars* 100 μm (**a-d**), 500 μm (**e-g**)

studied whether ARID1A undergoes a post-translational modification in vivo. We performed immunoprecipitation (IP) of ARID1A from ES cell lysates in the presence of NEM, an inhibitor of small ubiquitin-like modifier (SUMO) and ubiquitin isopeptidases. We found that ARID1A was indeed ubiquitinated as shown by immunoblotting with anti-ARID1 and anti-ubiquitin antibodies (Fig. 3d, lane 2). Similarly the immunoprecipitant from the anti-ubiquitin antibody produced the same high molecular weight band as that observed with the IP with anti-ARID1A (Fig. 3d, lane 3). Importantly, this band was undetected when IP was carried out in the absence of NEM (Fig. 3d, lanes 5, 6). These data confirmed that ARID1A was ubiquitinated in vivo in ES cells and probably in embryos. Immunoblotting of the IP of ARID1A with anti-SUMO antibody did not yield detectable bands of the expected size, suggesting that this protein was not sumoylated in ES cells.

Previous experiments have demonstrated that the ARID1 subunits function as part of an ubiquitin ligase that targets histone H2B (Li et al. 2010). Both proteins contain the characteristic motif of the E3 ubiquitin ligases known as the BC box domain. Mutation in the BC box of ARID1B results in its auto-ubiquitination and degradation in a proteasome-dependent manner. These data, together with our present observation, suggest that the stability of the ARID1 subunits might be regulated through ubiquitination.

Cell-cycle-regulated expression of ARID1 subunits in MC3T3 cells

Given that distinct functions have been demonstrated for ARID1A and ARID1B in the MC3T3-E1 cells in the regulation of the cell cycle, we were interested to determine whether the activities of these proteins were regulated in a cell-cycle-dependent manner. Nagl and colleagues (2007) have demonstrated that both ARID1A and ARID1B complexes directly bind to promoters of the cell cycle genes, viz., *cdc2*, *Cyclin A*, *Cyclin E*, and *c-Myc*, although their timing of promoter occupation is different. In cells synchronized by the deprivation of serum, complexes containing ARID1B are present in the promoters at all times from G0 to S phase, whereas complexes containing ARID1A are bound to the promoters at G0 when all these genes are repressed and dissociate as cells enter the S phase and genes start to be activated. These observations suggest

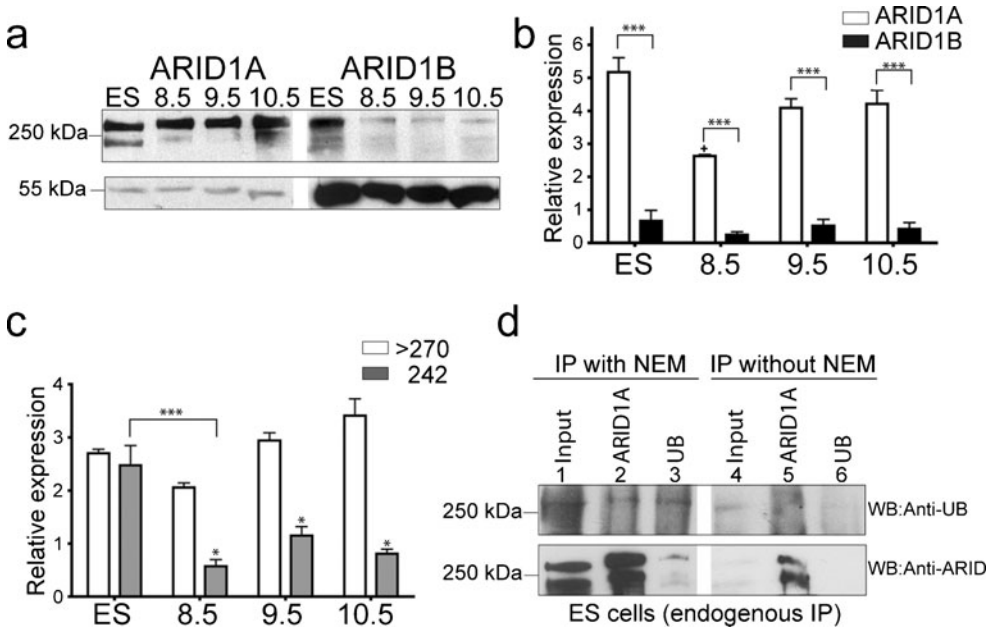

Fig. 3 Immunoblot analysis of the composition and protein levels of the ARID1 subunit isoforms in embryos. **a** Protein extracts prepared from embryos at the indicated stage and in embryonic stem (ES) cells resolved by SDS-polyacrylamide gel electrophoresis were tested with anti-ARID1A or anti-ARID1B antibodies and with anti-β-tubulin antibodies as the loading control. *Numbers left* indicate the molecular weight (*kDa*) of a protein ladder. **b** Densitometric analysis of the total amounts of ARID1A and ARID1B detected in the immunoblots. Data represent means of three independent measurements±SE; *t*-test, ***$P<0.005$, $^{+}P<0.05$, relative to ARID1A in ES cells. **c** Densitometric analysis comparing the relative amounts of the two indicated ARID1A bands at various developmental stages. Means±SE; *t*-test, ***$P<0.005$, *$P<0.05$, relative to 242 kDa in 8.5 dpc embryos. **d** ES cell lysates were immunoprecipitated (*IP*) with the indicated antibodies in TLB buffer, either in the presence or in the absence of N-ethylmaleimide (*NEM*) and subjected to Western blotting (*WB*; *UB* ubiquitin)

the possibility that conditions such as the availability of the ARID1 subunits, their association to nuclear components, or their interaction with other subunits of the complex might be regulated by differential synthesis or post-translational modifications. To explore these ideas, we used immunocytochemistry and Western blot to compare the expression of ARID1A and ARID1B during the various phases of the cell cycle in MC3T3-E1 cells.

In order to detect variations in the amount of the ARID1 proteins through interphase (G1 and S phases), we synchronized MC3T3-E1 cells by serum deprivation. After 3 days, serum was reintroduced, and cells were collected at t0 (G0/G1) and after 24 h (S) for double-immunostaining with anti-PCNA and anti-ARID1A or anti-ARID1B. Quantification of the intensity of the immunofluorescent signal was used as a relative measurement of the level of expression of the proteins in a number of cells. Through these experiments, we found that the level of signal for ARID1A did not vary significantly between PCNA-negative (G0/G1) and PCNA-positive (G1/S) cells (Fig. 4a-b, e-f); in contrast, the level of ARID1B protein increased as the cells entered S phase (Fig. 4c-d, g-h). As a continuation of this analysis, mitotic cells were identified in non-synchronized cells with the H3S10P antibody. Double-immunostaining of cells with anti-H3S10P and anti-ARID1 proteins showed that ARID1A was significantly down-regulated at prophase and completely degraded by metaphase (Fig. 5a, c), whereas ARID1B was not significantly reduced in mitotic cells, although it was excluded from condensed chromosomes (Fig. 5b, c). This evaluation indicated that the dynamics of ARID1A and ARID1B differed, both at interphase and at mitosis. ARID1A is synthesized at G0, and its level decreases throughout the cell cycle, whereas ARID1B remains present during all cell cycle phases. To document further the variations of ARID1A and ARID1B levels during mitosis, we undertook this same analysis in ES cells. Double-immunostaining of ES cell colonies with anti-H3S10P and anti-ARID1A or anti-ARID1B showed that ARID1A was also absent during mitosis in these cells (Fig. 5d, f). On the other hand, the level of ARID1B showed a moderate decrease in mitotic cells but remained present, even in anaphase and telophase during which its signal was detected surrounding the chromosomes (Fig. 5e, f). These findings indicate that the observed phenomenon is not cell-type specific.

We went on to see whether the ARID1 subunits had a similar dynamics of expression in vivo; to this end, we analyzed the distribution of the ARID1 proteins in mouse pre-implantation embryos. The same result as in cell culture was found for ARID1A in both morulas and blastocysts

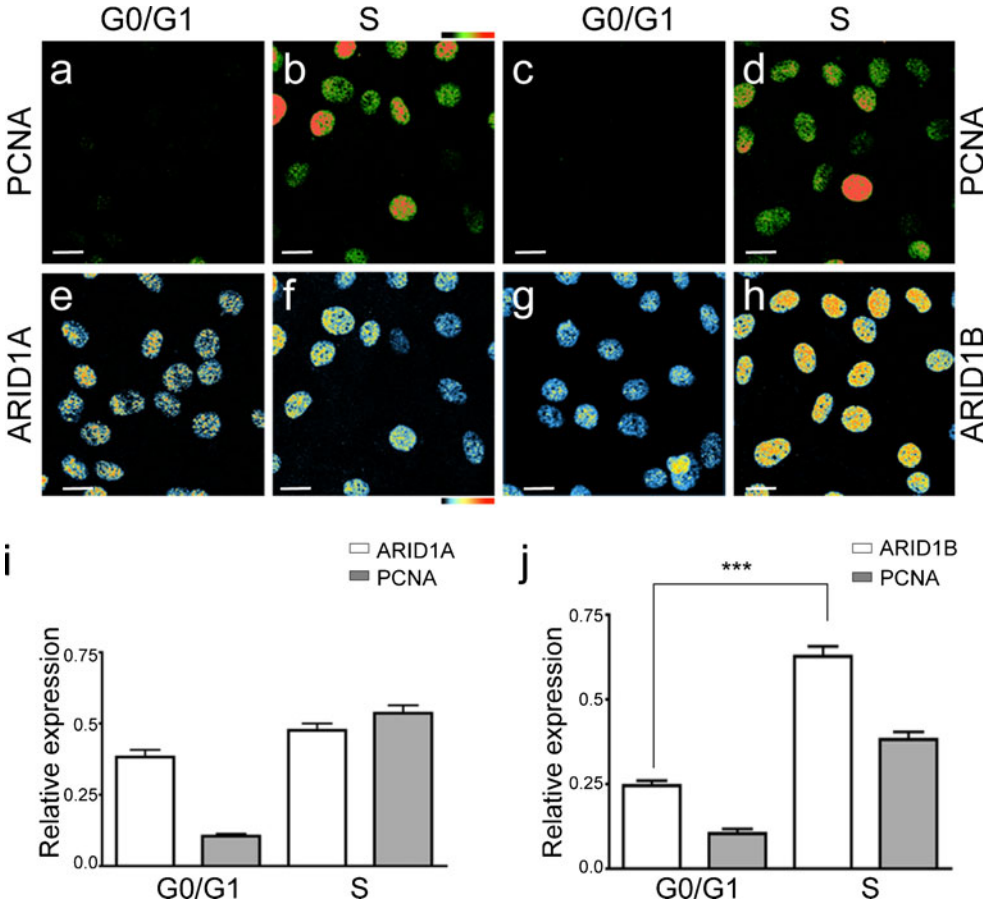

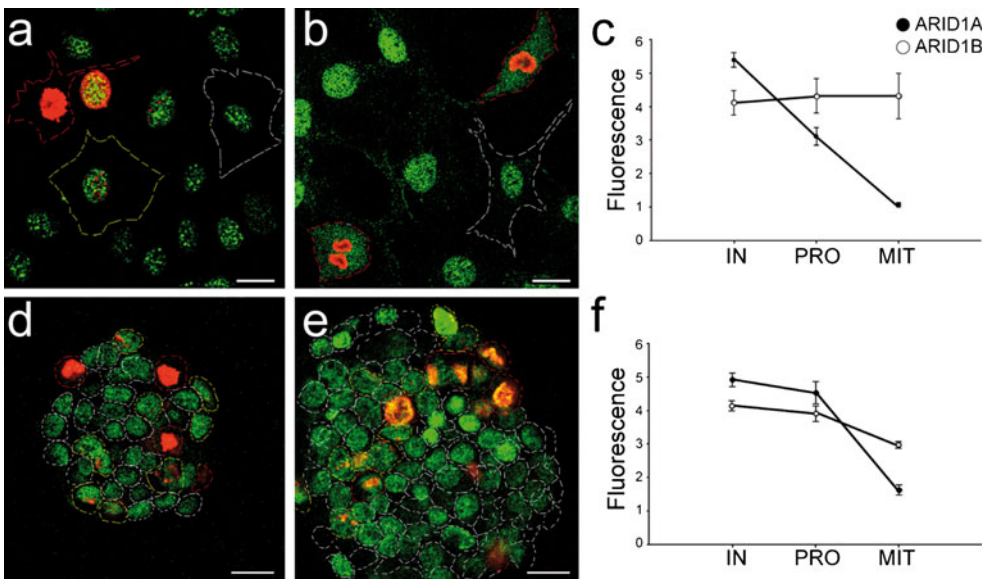

Fig. 4 Expression levels of ARID1A and ARID1B in interphasic cells. Immunofluorescent double detection of PCNA (**a-b**) and ARID1A (**e-f**), or PCNA and ARID1B (**c-d** and **g-h** respectively) in MC3T3 cells at G0/G1 (t0) and S (t24) phase. Fluorescence was represented with pseudocolor according to intensity of signal. Color-scale range 0-255 pixels, low (black) to high (red). (**i-j**) Quantification of fluorescence was done for at least 40 cells per experiment and the average plotted. Data represent means of three independent experiments ±SE. t test ***($p < 0.005$)

Fig. 5 Expression levels of ARID1A and ARID1B in mitotic cells. **a**, **b** Confocal merged images showing the double-immunofluorecent detection of the ARID1 proteins (*green*) and Ser10 phosphorylated histone 3 (H3S10P, *red*) in MC3T3 cells (**a** ARID1A, **b** ARID1B). *Bars* 20 μm. **c** Pixel intensity was quantified in MC3T3 cells for at least 40 cells and plotted as a function of the cell cycle phase. Data represent means of three independent experiments±SE (*IN* interphase, *PRO* prophase, *MIT* advanced mitosis). **d**, **e** Confocal merged images showing the double-immunofluorecent detection of the ARID1 proteins (*green*) and H3S10P (*red*) in ES cells (**d** ARID1A, **e** ARID1B). *Bars* 20 μm. Cells edges are delineated in *white* for interphasic cells, in *yellow* for prophasic cells, and in *red* for cells in advanced mitosis. **f** Fluorescence quantification for ES cells was performed as described in **c**

(Fig. 6a-b, e-f, i). Moreover, ARID1B was detected for the first time in eight-cell morulas (Fig. 6c, g); nonetheless, in blastomeres at prophase in these embryos, ARID1B was co-expressed with H3S10P (Fig. 6d, h, j) indicating its presence at this early mitotic phase. Again, ARID1B was found to be present in mitotic cells of the blastocyst.

With the aim of defining whether different isoforms of the ARID1 proteins could be detected at different cell cycle phases, Western blotting analysis was performed on protein extracts obtained from synchronized cells. A different protocol was used for synchronization in order to achieve the maximal enrichment of the corresponding cell cycle phases. Serum deprivation for 3 days was used to block cells at G1; for S phase arrest, exponentially growing cells were blocked with hydroxyurea for 18 h and released into fresh medium with serum for 3 h. Alternatively, cells released from the hydroxyurea block were treated for 24 h with colchicine for enrichment of G2/M cells (Fig. 7a). Synchronized cells were collected for flow cytometry and protein extraction. This analysis revealed that the ARD1A antibody only detected a 270-kDa band in the MC3T3-E1 line in all the cell cycle phases (Fig. 7b). Quantification of this band confirmed that the ARID1A presented its maximal level of expression at G0/G1 and decreased over the G1/S phase transition, reaching its lowest level at G2/M (Fig. 7b, c). These kinetics correlated with the reported

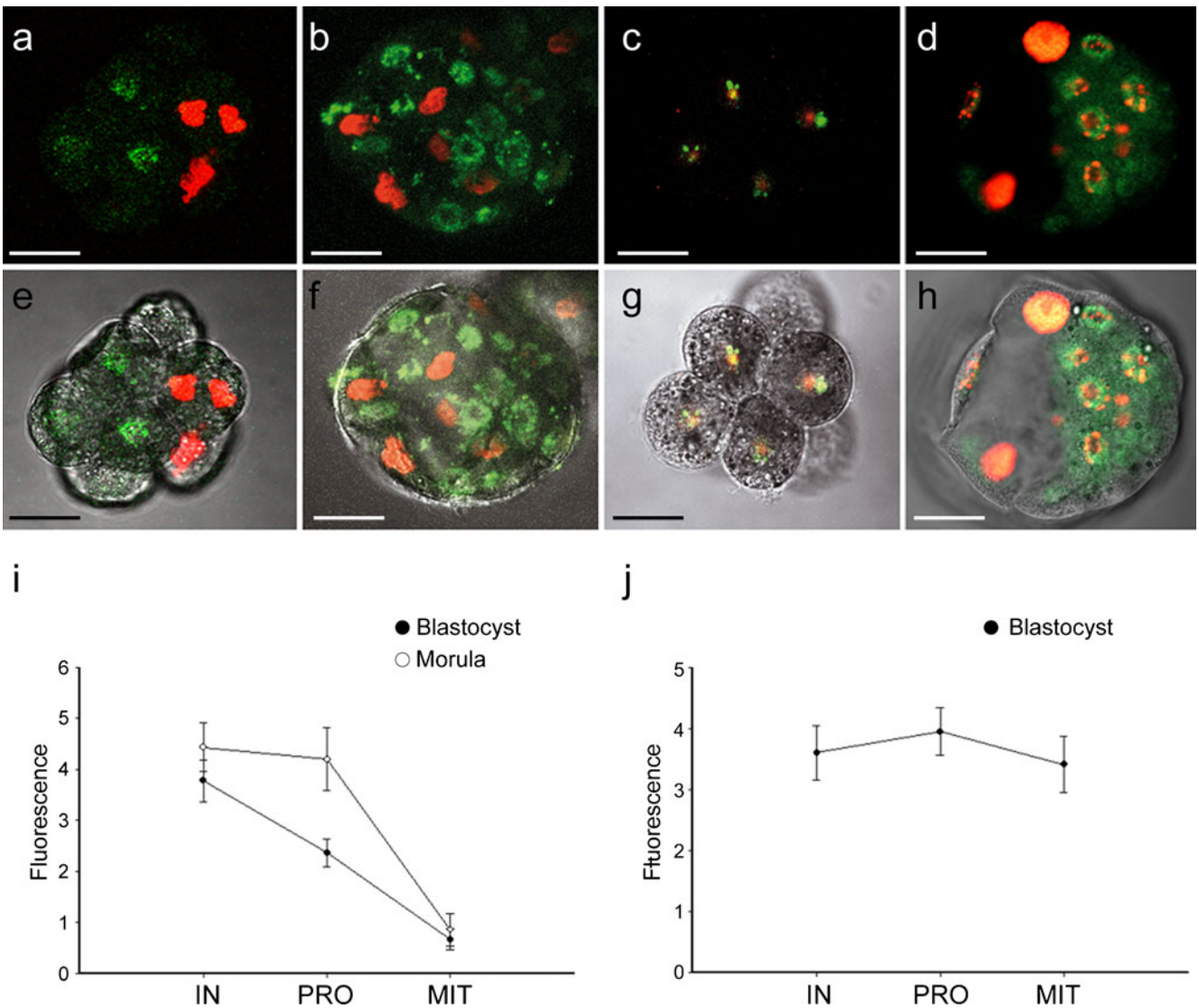

Fig. 6 Immunofluorescent localization of ARID1A and ARID1B in pre-implantation embryos. Confocal merged images of co-immunofluorescence (**a**, **b**, **e**, **f**) with anti-ARID1A (*green*) and anti-H3S10P (*red*), in a morula (**a**, **e**) and a blastocyst (**b**, **f**) or (**c**, **d**, **g**, **h**) with anti-ARID1B (*green*) and anti-H3S10P (*red*) in a morula (**c**, **g**) and a blastocyst (**d**, **h**). Merged images (**e-h**) of immunofluorescence (**a-d**) plus bright field images. *Bars* 20 μm. Quantification of pixel intensities for at least 40 cells was plotted as a function of the cell cycle phase (*IN* interphase, *PRO* prophase, *MIT* advanced mitosis) for ARID1A (**i**) and for ARID1B (**j**). For ARID1B, expression in the morula was low and therefore was not quantified. Data represent means of three independent experiments±SE

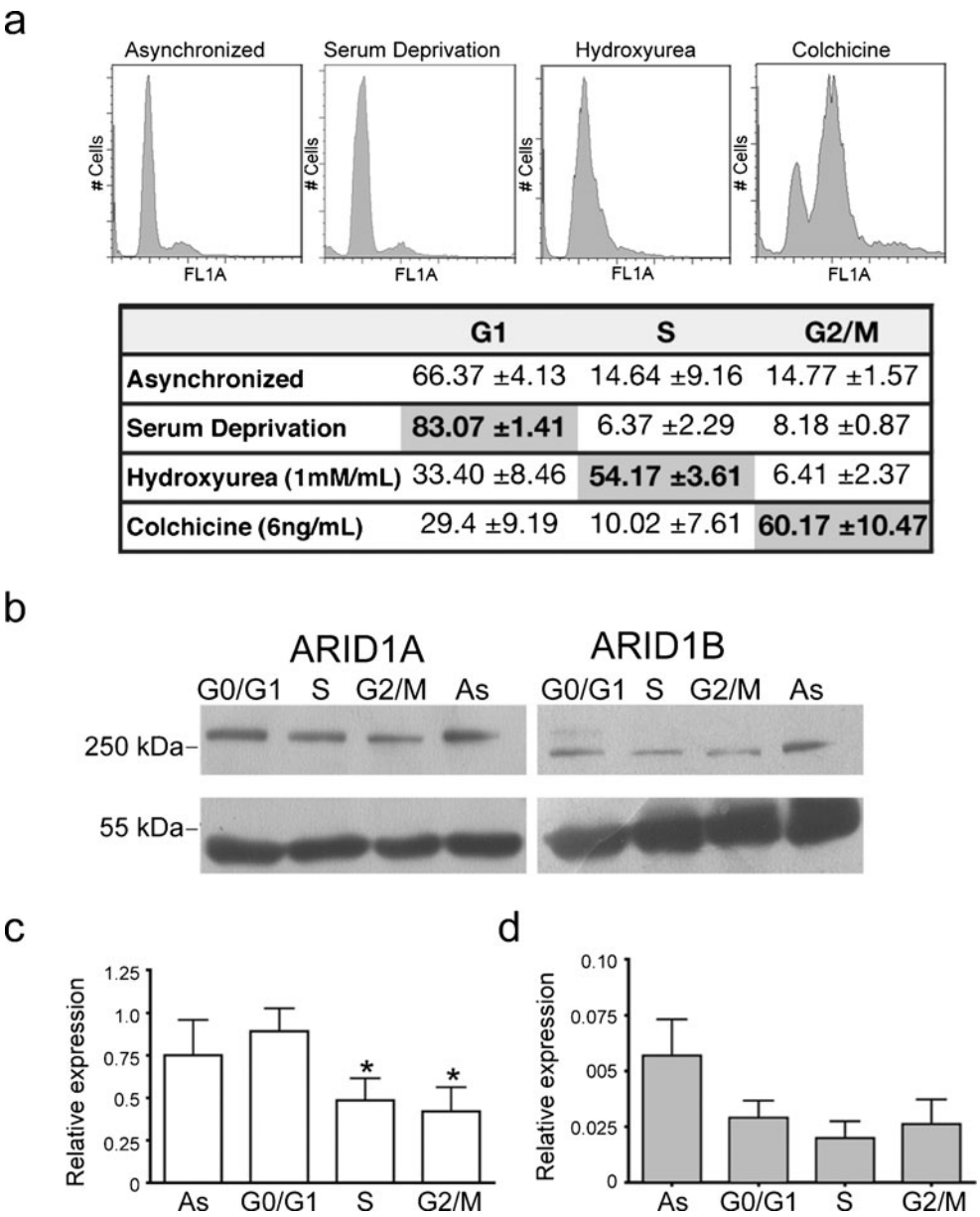

	G1	S	G2/M
Asynchronized	66.37 ±4.13	14.64 ±9.16	14.77 ±1.57
Serum Deprivation	**83.07 ±1.41**	6.37 ±2.29	8.18 ±0.87
Hydroxyurea (1mM/mL)	33.40 ±8.46	**54.17 ±3.61**	6.41 ±2.37
Colchicine (6ng/mL)	29.4 ±9.19	10.02 ±7.61	**60.17 ±10.47**

Fig. 7 Isoform composition and expression levels of ARID1A and ARID1B in synchronized MC3T3-E1 cells. **a** Fluorescence-activated cell sorting (FACS) analysis after the staining of DNA with Sytox-green. FACS was performed for the asynchronous cell population or for cells after the indicated treatments. The distribution of cells in the cell cycle after each treatment is indicated in the table as percentages. **b** Western immunoblot analysis of cell extracts from asynchronous cells (*As*) or cells enriched with the indicated cell cycle phase populations. **c**, **d** Densitometric analysis comparing the relative amounts of ARID1A and ARID1B, respectively, detected in the immunoblot. Normalization with β-tubulin levels was performed. Data represent means of three independent experiments +/−SE ; *t*-test, **P*<0.05 relative to G0/G1

dynamics of dissociation of ARID1A from cell cycle promoters in S phase (Nagl et al. 2007). Immunoblotting analysis for ARID1B indicated that this protein exhibited different kinetics from that of ARID1A, being expressed at a comparable level in all phases (Fig. 7b, d). The anti-ARID1B antibody detected a 239-kD band in all protein samples, and a higher molecular weight species was detected at G0/G1, similar to that observed in embryo extracts. This antibody also detected a 120-kDa band in all cell cycle phases (not shown). Because this species was present constantly in the MC3T3-E1 cell line and was not detected in embryo extracts, we consider that it is not an intermediate proteolytic product of the degradative machinery, but rather that it represents a specific product from post-translational proteases processing. The possibility that this shorter species is functional in this cell line cannot be discarded.

Discussion

We have examined the embryonic pattern of expression of the *Arid1a* and *Arid1b* genes. These genes encode for subunits that selectively incorporate into the SWI/SNF remodeling complex providing it with antagonistic functions during cell proliferation. A comparison of their expression patterns indicates that *Arid1a* is intensively produced and widely distributed over the embryo, whereas *Arid1b* presents a weaker and more restricted expression. *Arid1b* is predominantly expressed in neural tissues,

suggesting that it is important for the early development of the brain when multipotent neuroepithelial cells are actively proliferating. *Arid1a* is also strongly expressed in these same regions, perhaps in the same cells. Chromatin-remodeling events have been shown to be critically important during neural development (Lessard et al. 2007; Ho and Crabtree 2010). Thus, the presence of both subunits in neural tissues is in agreement with the increased variety of specific complexes required for greater functional diversity.

The immunoblot analysis has demonstrated that, at the protein level, a similar ratio of a molar excess of ARID1A over ARID1B is observed, suggesting that ARID1A is constantly participating in SWI/SNF activity in the embryo. We have also found that both ARID1 subunits present a size increase, and for ARID1A, we have confirmed that this is attributable to ubiquitin modification. In embryos, most of the ARID1A protein consistently migrates as the ubiquitin-modified form, whereas in ES cells, a more significant amount of the total protein migrates as an unmodified species. This result suggests that ubiquitination of the ARID1A protein is regulated during embryo development.

Because of the opposite roles of the ARID1 proteins during the cell cycle in MC3T3-E1 cells, we have also studied their kinetics of expression throughout the cell cycle phases. Using immunocytochemistry, we have found that they exhibit different kinetics. ARID1A is accumulated at G0 phase, and its level does not change significantly after serum stimulation, but it appears to be degraded when cells enter mitosis. In contrast, ARID1B increases in response to serum and remains stable at mitosis. Importantly, in ES cells and pre-implantation embryos in which only the S and M phases occur, a similar behavior is found at mitosis, implying that this differential degradation is not a peculiarity of the MC3T3 line but could be of biological significance. Our immunoblot studies at interphase have confirmed that the level of ARID1A decreases over the cell cycle, whereas that of ARID1B remains constant; however, the results of these experiments show some differences compared with the data obtained by IF. The Western blots indicate that ARID1A is significantly lost as early as during the G1/S phase transition and continues to decrease up to the G2/M phase. In addition, this analysis has not revealed an increase of the ARID1B level in response to serum. These discrepancies can be explained (1) in terms of the different protocols used for synchronization, and (2) because, in the IF assay, double-staining allows a distinction of cells at specific cell cycle phases. Thus, whereas the Western blot yields more precise quantification, purer populations are considered in the IF. Regardless of the different approaches used, we can conclude that ARID1A accumulates in G0 and is downregulated throughout the cell cycle, probably by proteolysis. On the other hand, ARID1B is not eliminated through the cell cycle, because it is more resistant to proteolysis, because it is synthesized after serum stimulation, or both. Degradation of ARID1A might be a way of regulating the binding of this protein to its target promoters and facilitating the binding of ARID1B, which is permanently available but at much lower concentrations.

The expression levels of human BRM and BRG-1 at the various phases of the cell cycle have previously been followed (Muchardt et al. 1996): BRM presents similar kinetics to those found here for ARID1A, whereas the level of BRG-1 remains constant throughout the cell cycle, as we describe for ARID1B. These similarities could be significant in the light of recent evidence suggesting that, among the four different combinations of the ARID1 subunits and ATPases, BRM/ARID1A complexes are found more often in repressed promoters, while BRG1/ARID1B complexes are found more often in active promoters (Flowers et al. 2009; Kaeser et al. 2008). Thus, the kinetics of expression during the cell cycle could contribute to the regulation of the incorporation patterns of those SWI/SNF subunits that are mutually exclusive paralogs.

In conclusion, we have shown that ARID1A is more significantly expressed through embryonic development than ARID1B and that the levels of these proteins are regulated during the cell cycle suggesting that their availability during the various cell cycle phases might be relevant for the combinatorial assembly of the complex and for the modulation of the function of SWI/SNF during proliferation and arrest.

Acknowledgements We thank Andrés Saralegui for assistance with the confocal microscopy, Dr. Enrique Salas for assistance in work with preimplantation embryos, Aimée Bastidas and David Hernández for assistance with ES culture, María Elena Bravo-Adame and Erika Melchy for assistance in the cell sorting, and Marcela Ramírez for assistance with mice.

References

Dallas PB, Pacchione S, Wilsker D, Bowrin V, Kobayashi R, Moran E (2000) The human SWI-SNF complex protein p270 is an ARID family member with non-sequence-specific DNA binding activity. Mol Cell Biol 20:3137–3146

Flowers S, Nagl NG Jr, Beck GR Jr, Moran E (2009) Antagonistic roles for BRM and BRG1 SWI/SNF complexes in differentiation. J Biol Chem 284:10067–10075

Gao X, Tate P, Hu P, Tjian R, Skarnes WC, Wang Z (2008) ES cell pluripotency and germ-layer formation require the SWI/SNF chromatin remodeling component BAF250a. Proc Natl Acad Sci USA 105:6656–6661

Ho L, Crabtree GR (2010) Chromatin remodelling during development. Nature 463:474–484

Hogan B, Beddington R, Costantini F, Lacy E (1994) Manipulating the mouse embryo: a laboratory manual. Cold Spring Harbor Laboratory, Cold Spring Harbor, NY

Hurlstone AF, Olave IA, Barker N, Noort M van, Clevers H (2002) Cloning and characterization of hELD/OSA1, a novel BRG1 interacting protein. Biochem J 364:255–264

Kaeser MD, Aslanian A, Dong MQ, Yates JR 3rd, Emerson BM (2008) BRD7, a novel PBAF-specific SWI/SNF subunit, is required for target gene activation and repression in embryonic stem cells. J Biol Chem 283:32254–32263

Kozmik Z, Machon O, Kralova J, Kreslova J, Paces J, Vlcek C (2001) Characterization of mammalian orthologues of the *Drosophila* osa gene: cDNA cloning, expression, chromosomal localization, and direct physical interaction with Brahma chromatin-remodeling complex. Genomics 73:140–148

Lessard J, Wu JI, Ranish JA, Wan M, Winslow MM, Staahl BT, Wu H, Aebersold R, Graef IA, Crabtree GR (2007) An essential switch in subunit composition of a chromatin remodeling complex during neural development. Neuron 19:201–215

Li XS, Trojer P, Matsumura T, Treisman JE, Tanese N (2010) Mammalian SWI/SNF—a subunit BAF250/ARID1 is an E3 ubiquitin ligase that targets histone H2B. Mol Cell Biol 30:1673–1688

Martens JA, Winston F (2003) Recent advances in understanding chromatin remodeling by Swi/Snf complexes. Curr Opin Genet Dev 13:136–142

Mohrmann L, Verrijzer CP (2005) Composition and functional specificity of SWI2/SNF2 class chromatin remodeling complexes. Biochim Biophys Acta 1681:59–73

Muchardt C, Reyes JC, Bourachot B, Leguoy E, Yaniv M (1996) The hbrm and BRG-1proteins, components of the human SNF/SWI complex, are phosphorylated and excluded from the condensed chromosomes during mitosis. EMBO J 15:3394–3402

Nagl NG Jr, Patsialou A, Haines DS, Dallas PB, Beck GR Jr, Moran E (2005) The p270 (ARID1A/SMARCF1) subunit of mammalian SWI/SNF-related complexes is essential for normal cell cycle arrest. Cancer Res 65:9236–9244

Nagl NG Jr, Zweitzig DR, Thimmapaya B, Beck GR Jr, Moran E (2006) The c-myc gene is a direct target of mammalian SWI/SNF-related complexes during differentiation-associated cell cycle arrest. Cancer Res 66:1289–1293

Nagl NG Jr, Wang X, Patsialou A, Van Scoy M, Moran E (2007) Distinct mammalian SWI/SNF chromatin remodeling complexes with opposing roles in cell-cycle control. EMBO J 26:752–763

Nie Z, Yan Z, Chen EH, Sechi S, Ling C, Zhou S, Xue Y, Yang D, Murray D, Kanakubo E, Cleary ML, Wang W (2003) Novel SWI/SNF chromatin-remodeling complexes contain a mixed-lineage leukemia chromosomal translocation partner. Mol Cell Biol 23:2942–2952

Ryme J, Asp P, Bohm S, Cavellan E, Farrants AK (2009) Variations in the composition of mammalian SWI/SNF chromatin remodelling complexes. J Cell Biochem 108:565–576

Wang W (2003) The SWI/SNF family of ATP-dependent chromatin remodelers: similar mechanisms for diverse functions. Curr Top Microbiol Immunol 274:143–169

Wang X, Nagl NG Jr, Flowers S, Zweitzig D, Dallas PB, Moran E (2004a) Expression of p270 (ARID1A), a component of human SWI/SNF complexes, in human tumors. Int J Cancer 112:636

Wang X, Nagl NG, Wilsker D, Van Scoy M, Pacchione S, Yaciuk P, Dallas PB, Moran E (2004b) Two related ARID family proteins are alternative subunits of human SWI/SNF complexes. Biochem J 383:319–325

Yan Z, Wang Z, Sharova L, Sharov AA, Ling C, Piao Y, Aiba K, Matoba R, Wang W, Ko MS (2008) BAF250B-associated SWI/SNF chromatin-remodeling complex is required to maintain undifferentiated mouse embryonic stem cells. Stem Cells 26:1155–1165